

# Model Fractional Chern Insulators

Jörg Behrmann,<sup>1</sup> Zhao Liu,<sup>1,2,\*</sup> and Emil J. Bergholtz<sup>1,†</sup>

<sup>1</sup>*Dahlem Center for Complex Quantum Systems and Institut für Theoretische Physik,  
Freie Universität Berlin, Arnimallee 14, 14195 Berlin, Germany*

<sup>2</sup>*Department of Electrical Engineering, Princeton University, Princeton, New Jersey 08544, USA*  
(Dated: May 31, 2016)

We devise local lattice models whose ground states are *model fractional Chern insulators*—Abelian and non-Abelian topologically ordered states characterized by exact ground state degeneracies at any finite size and infinite entanglement gaps. Most saliently, we construct exact parent Hamiltonians for two distinct families of bosonic lattice generalizations of the  $\mathbb{Z}_k$  parafermion quantum Hall states: (i) color-entangled fractional Chern insulators at band filling fractions  $\nu = k/(\mathcal{C} + 1)$  and (ii) nematic states at  $\nu = k/2$ , where  $\mathcal{C}$  is the Chern number of the lowest band. In spite of a fluctuating Berry curvature, our construction is partially frustration free: the ground states reside entirely within the lowest band and exactly minimize a local  $(k+1)$ -body repulsion term by term. In addition to providing the first known models hosting intriguing states such as higher Chern number generalizations of the Fibonacci anyon quantum Hall states, the remarkable stability and finite-size properties make our models particularly well-suited for the study of novel phenomena involving e.g. twist defects and proximity induced superconductivity, as well as being a guide for designing experiments.

PACS numbers: 73.43.Cd, 03.75.Mn

**Introduction.** The prospect of lattice-scale fractional quantum Hall (FQH) phenomena at high temperatures, without the need for a strong magnetic field, has attracted ample recent attention to the theory of fractional Chern insulators (FCIs) [1–3]. While experimental realizations of FCIs are becoming increasingly realistic in the light of the recent realizations of integer Chern insulators with unit Chern number in solid state materials [4] and cold atom systems [5], the theoretical frontier has turned towards strongly correlated states in bands with higher Chern numbers [6–27]. This is due to the fact that, although notable differences compared to the continuum setting have been established [2, 28, 29], all FCIs discovered in Chern number  $\mathcal{C} = 1$  bands have direct continuum FQH analogs to which the adiabatic continuity has been explicitly established in several important cases [30–35]. Of special value is the early work by Kapit and Mueller who provided a natural lattice discretization of the continuum lowest Landau level and showed that an two-body on-site interaction leads to a perfect lattice version of the bosonic  $\nu = 1/2$  Laughlin state [30]. Related work has established the existence lattice parent Hamiltonians of non-Abelian states [36–38].

There is however a glaring lack of similar models describing  $\mathcal{C} > 1$  systems, despite intriguing progress with long-ranged lattice models [39] and approximative mappings to continuum models with unusual boundary conditions [14]. Given the importance of solvable models in the theory of topological and strongly correlated states of matter—ranging from the AKLT model for the Haldane spin chain [40] and the Kitaev chain describing a one-dimensional  $p$ -wave superconductor [41] to the model wave functions for the continuum FQH effect [42–44] and their concomitant pseudopotential parent Hamiltonians [45]—finding such has remained an outstanding challenge in the theory of FCIs. This is particularly pressing given the accumulating numerical evidence that  $\mathcal{C} > 1$  sys-

tems feature an even richer phenomenology than continuum Landau levels.

In the present work, we bridge this divide and provide exact lattice parent Hamiltonians for a large class of Abelian as well as non-Abelian *model* FCIs in bands carrying any Chern number  $\mathcal{C}$ . We explicitly verify that the ground state multiplets are exactly degenerate at any finite size, that the gap to excited states remains finite in the thermodynamic limit, and that there is an infinite gap in the particle entanglement spectrum [46, 47].

**Flat band model.** We begin by constructing a family of multi-orbital models possessing exactly flat lowest bands with arbitrary Chern number  $\mathcal{C}$ . For definitiveness we describe our construction on a square lattice with an effective magnetic flux  $\phi = 1/q$  piercing each elementary plaquette [48], although it can be generalized to any Bravais lattice and rational flux.

We assign  $M$  internal orbitals to each lattice site  $i$  with real-space coordinates  $(x_i, y_i)$ , where  $M$  must be a factor of  $q$ . The site-dependent orbital index to the lattice site  $i$  is  $s_i = x_i \bmod (\frac{q}{M}) + m \frac{q}{M}$ , with  $m = 0, 1, \dots, M - 1$ . The single-particle physics is governed by

$$H_0 = \sum_{j,s_j} \sum_{k,s_k} t_{j,k}^{s_j,s_k} a_{j,s_j}^\dagger a_{k,s_k}, \quad (1)$$

where  $a_{j,s_j}^\dagger$  ( $a_{j,s_j}$ ) creates (annihilates) a particle on the orbital  $s_j$  at site  $j$ . To achieve an exactly flat lowest Chern band we choose the hopping amplitudes as [49]

$$t_{j,k}^{s_j,s_k} = \delta_{s_j - x_j, s_k - x_k}^{\bmod q} (-1)^{x+y+xy} e^{-\frac{\pi}{2}(1-\phi)|z|^2} e^{-i\pi\phi(\tilde{x}_j + \tilde{x}_k)y}, \quad (2)$$

where  $z_j = x_j + iy_j$ ,  $z = z_j - z_k$ , and  $\tilde{x}_j = x_j + (s_j - x_j) \bmod q$ . The hopping amplitudes decay as a function of the distance between site  $k$  and site  $j$  like a Gaussian. The hopping phase factor depends on both  $x_i$  and  $s_i$  according to the definition of  $\tilde{x}_i$ . The unit cell of our model contains

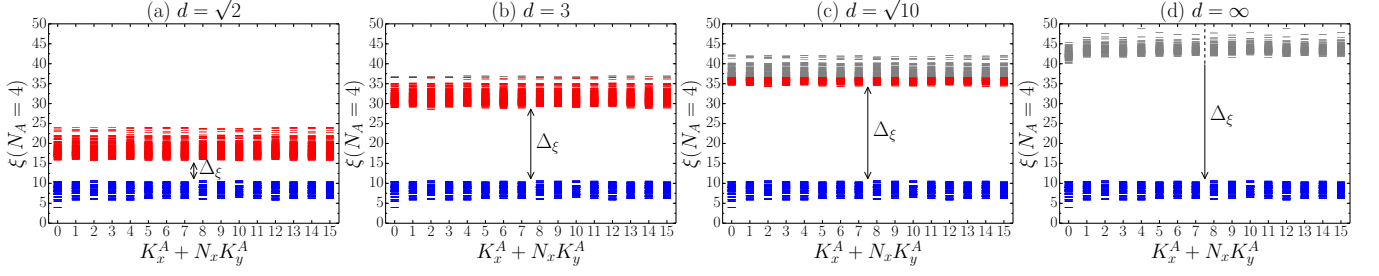


Figure 1. (Color online) Typical particle entanglement spectra (PES), here displayed for the  $k = 2, \nu = 2/3$  non-Abelian state in a  $\mathcal{C} = M = 3$  band with  $N = 8, N_x \times N_y = 4 \times 4, \phi = 1/3$  and hoppings truncated at (a)  $d = \sqrt{2}$ , (b)  $d = 3$ , (c)  $d = \sqrt{10}$ , and (d)  $d = \infty$  lattice constants. Generally a PES obtained by numerical diagonalization includes three parts: the low-lying levels with quasihole excitation information (blue), the high non-universal levels (red), and numerical noise (gray) set by the double precision above  $\xi_c \approx \ln(2^{-53}) \approx 36.7$ . The high, non-universal levels merge into numerical noise for large  $d$ , preventing us from further numerically tracking the growth of the entanglement gap, which we argue to increase without bound with increasing  $d$ .

$q/M$  sites in the  $x$  direction. The  $q$  orbitals in a unit cell lead to  $q$  bands, and the lowest thereof is exactly flat and carries Chern number  $\mathcal{C} = M$ . For  $M = 1$ , our construction Eqs. (6) and (7) reduces to the Kapit-Mueller model [30] in Landau gauge. Similar multi-orbital models have also been studied in Refs. [10, 18] albeit with different choices for the hopping amplitudes.

Although it is generally impossible to have an exactly flat band with non-zero Chern number and strictly finite hopping [50], our model is local in the sense of being at least exponentially bounded. Truncating the hopping at a distance of  $d = 2$  lattice constants already gives a high flatness ratio between the band gap and bandwidth: e.g. for  $\phi = 1/6$  and  $\mathcal{C} = 2$  or 3 one finds  $f \approx 85$  or 73 respectively. The efficiently quenched kinetic energy amplifies the importance of interaction effects and we will now proceed to show that local interactions indeed generate model FCIs.

**Color-entangled FCIs.** We begin by considering  $N$  particles with the  $(k + 1)$ -body on-site repulsion on a finite lattice of  $N_x \times N_y$  unit cells with periodic boundary conditions. The interaction Hamiltonian reads

$$H_{\text{int}} = \sum_i \sum_{\sigma_0 \leq \sigma_1 \leq \dots \leq \sigma_k \in \{s_i\}} :n_{i,\sigma_0} n_{i,\sigma_1} \dots n_{i,\sigma_k}:, \quad (3)$$

where  $n_{i,\sigma}$  is the occupation operator on the orbital  $\sigma$  at lattice site  $i$ , and  $: \dots :$  enforces the normal ordering. For  $\mathcal{C} = M = 1$ , the single-particle wave functions of the lowest band of Eq. (6) have the structure of a discretized lowest Landau level, and lattice analogs of the  $\mathcal{Z}_k$  Read-Rezayi states are unique zero-energy ground states of Eq. (3) at  $\nu = N/(N_x N_y) = k/2$  up to an exact  $(k + 1)$ -fold degeneracy, when the number of particles is a multiple of  $k$ , because the exact clustering properties of these wave functions [44] carry over directly to the present lattice setting. This is astonishing given that many other properties such as the fluctuating Berry curvature in reciprocal space and the excitation spectrum already deviate from that in the continuum since the discretized Landau level orbitals are non-orthogonal. Furthermore, if the wave functions are written in a properly orthogonalized Wannier basis [31–33], they

differ from the continuum model states [19, 38]. Nevertheless, we find that these states are characterized by an infinite gap in the particle entanglement spectrum (PES) which probes the quasihole excitations of the system [46, 47]. Remarkably, we find that this scenario generalizes to any  $\mathcal{C} = M > 1$ : at filling fractions  $\nu = k/(\mathcal{C} + 1)$ , there are  $\binom{\mathcal{C}+k}{k}$ -fold exactly degenerate zero-energy ground states when the number of particles is a multiple of  $k$ , and their PES has an infinite gap.

To establish this, we project the interaction Hamiltonian Eq. (3) for large number of samples onto the lowest band, and compute the many-body eigenvalues and eigenstates by exact diagonalization. Indeed, we always observe the expected number of zero-energy modes in the energy spectrum [48, 51], which in turn implies that the band projection leaves the ground states unchanged. We also find the number of zero-energy modes is robust against the flux insertion (twisted boundary conditions). To demonstrate the infinite entanglement gap in the particle entanglement spectrum (PES), we truncate the hopping range in Eq. (6) at distance  $d$ , then track the evolution of the PES with increasing  $d$ . While the lowest band is dispersive for finite  $d$ , we study the band projected version thus ignoring the band dispersion. For a system of  $N$  particles described by the density matrix  $\rho = \frac{1}{\mathcal{D}} \sum_{\alpha=1}^{\mathcal{D}} |\Psi_\alpha\rangle \langle \Psi_\alpha|$ , where  $|\Psi_\alpha\rangle$  is the  $\alpha$ th state in the ground state manifold with degeneracy  $\mathcal{D}$  [52], the PES levels  $\xi$  are defined as  $\xi \equiv -\ln \lambda$ , where the  $\lambda$  are the eigenvalues of the reduced density matrix  $\rho_A$  of  $N_A$  particles obtained by tracing out  $N_B = N - N_A$  particles from the whole system, i.e.  $\rho_A = \text{Tr}_B \rho$  [47]. Each PES level can be labeled by the total two-dimensional quasi-momentum  $(K_x^A, K_y^A)$  of part  $A$ . When the PES levels are clearly divided into low-lying and higher excited parts, we define the entanglement gap as  $\Delta_\xi \equiv \xi_{i+1} - \xi_i$ , where  $\xi_i$  ( $\xi_{i+1}$ ) is the highest (lowest) level in the low-lying (excited) part.

Typical PES at different truncations are shown in Fig. 1 for the  $\nu = 1/2$  non-Abelian state in a  $\mathcal{C} = 3$  band. Including only nearest and next-nearest neighbor hopping, i.e.  $d = \sqrt{2}$  [Fig. 1(a)], we observe a clear entanglement gap of  $\Delta_\xi \approx 5$  which is already larger than most of previously reported re-

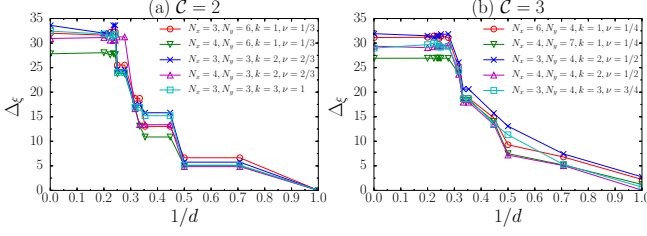


Figure 2. (Color online) The entanglement gap  $\Delta_\xi$  in the  $N_A = \lceil N/2 \rceil$  sector versus the inverse hopping distance  $1/d$  in (a)  $C = 2$  and (b)  $C = 3$  band. For each  $C$ , we consider both Abelian states at  $\nu = 1/(\mathcal{C} + 1)$  and non-Abelian states at  $\nu = 2/(\mathcal{C} + 1)$  and  $\nu = 3/(\mathcal{C} + 1)$ , with lattice geometry of either  $\gcd(N_x, C) = C$  or  $\gcd(N_x, C) = 1$ .  $\phi$  is chosen as  $1/C$ . For  $d$  longer than three or four lattice constants, the size of  $\Delta_\xi$  cannot be tracked further due to the limitation of machine precision.

sults in the literature [6, 12, 53]. Increasing  $d$  further elevates the non-universal part of the PES and quickly enlarges the entanglement gap [Figs. 1(b) and 1(c)]. Our capability of tracking the growth of the entanglement gap is only limited by the machine precision, which determines that the PES levels can be computed reliably at most up to  $\xi_c \approx 36.7$ , which corresponds to an exponentially small amplitude, of order  $\mathcal{O}(e^{-\xi_c/2})$ , in the ground state wave function. When the non-universal levels merge into the numerical noise, it is impossible to identify the entanglement gap [Fig. 1(d)] accurately. This happens when the machine error dominates the high-energy part in the PES, the entanglement gap has already grown to  $\Delta_\xi \approx 30$ , which is much larger than previously reported values. We observe a similar growth of the entanglement gap when  $1/d \rightarrow 0$  in all investigated samples, as shown in Fig. 2.  $\Delta_\xi$  reaches  $5 \lesssim \Delta_\xi \lesssim 7$  at  $d = \sqrt{2}$ , exceeding most of the previously reported results, and quickly increases to  $\Delta_\xi \approx 30$  at  $d \approx 4$ , where numerical noise starts to prevent us from further tracking the growth of  $\Delta_\xi$ . However, the rapid growing of  $\Delta_\xi$  and extrapolating the data to  $1/d = 0$  clearly suggest infinite entanglement gaps of model FCIs. A short-range truncation of Eq. (6) is enough to get FCIs which are essentially indistinguishable from model FCIs with infinite entanglement gaps.

While the ground states and quasi-hole excitations have identically zero interaction energy in our model, the gap  $\Delta_E$ —measured at fixed particle number corresponding to a particle-hole excitation pair—is in principle size-dependent. The projection of the interaction to the lowest band will not affect the many-body gap as long as the band gap is much larger than the interaction strength, since low-lying excitations are purely determined by the interaction and the projection, excluding excitations caused by hopping from lower to higher bands. In Fig. 3, we plot  $\Delta_E$  versus the inverse particle number  $1/N$  for various model FCIs. In each case we find that the gap clearly extrapolates to a finite value in the thermodynamic limit, and, compared to other FCI models, the gap is remarkably insensitive to the system size (cf. e.g. Ref. [28]).

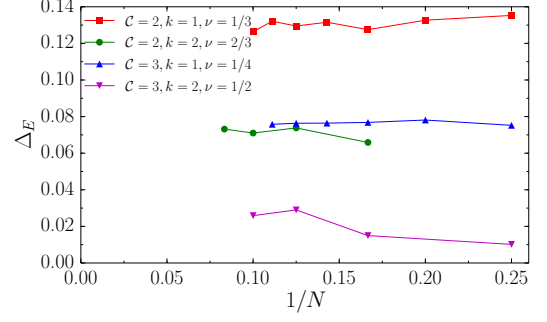


Figure 3. (Color online) The finite-size scaling of the energy gap for the Abelian  $\nu = 1/(\mathcal{C} + 1)$  states and non-Abelian  $\nu = 2/(\mathcal{C} + 1)$  states in  $C = 2$  and  $C = 3$  bands. Note that the spread of the ground state manifold is exactly zero here.  $N_x$  and  $N_y$  are appropriately chosen to make samples as isotropic as possible.  $\phi$  is chosen as  $1/C$ .

Having established the ideal nature of FCIs in our model, we now turn to its color-entangled nature. If we interpret  $m = 0, 1, \dots, M - 1$  in the orbital indices  $s_i$  as “layers” or “colors”, Eq. (6) on an infinite lattice is equivalent to a shifted stacking of  $M$  layers of the infinite  $M = 1$  model. However, for a *finite* lattice of  $N_x \times N_y$  unit cells with periodic boundary conditions, the corresponding stacking has color-entangled boundary conditions [7, 14, 18] in the  $x$ -direction in the sense that the hopping across the boundary may occur between orbitals belonging to different layers (usual periodic boundary conditions apply in the  $y$ -direction) [48]. Crucially, each layer is not necessarily a complete  $M = 1$  model with integer number of unit cells and periodic boundary conditions. Instead, one finds that Eq. (6) can be mapped to  $\gcd(N_x, M)$  copies of complete  $M = 1$  model with usual periodic boundary conditions. Ref. [14] provided a color-entangled basis built from continuum Landau levels and showed that provides a promising approach to the  $\nu = k/(\mathcal{C} + 1)$  FCIs by providing numerical evidence for a few states with small  $C$  and  $k$  [6, 12, 14]. When  $N_x$  is divisible by  $M$ , the FCIs correspond to color-dependent magnetic-flux inserted versions of the Halperin [54] or non-Abelian spin singlet states [55, 56]. Our construction extends this list of color-entangled FCIs and, by contrast, gives an exact construction directly in the real-space lattice.

*Nematic states.* The Hamiltonian Eq. (3) includes interactions within the same orbital and between different orbitals. Now we consider the zero-energy states in the presence of only on-site  $(k + 1)$ -body intra-orbital repulsion, i.e.

$$H_{\text{int}} = \sum_i \sum_{\sigma_0=\sigma_1=\dots=\sigma_k \in \{s_i\}} :n_{i,\sigma_0} n_{i,\sigma_1} \dots n_{i,\sigma_k}: \quad (4)$$

As discussed above, the single-particle problem can be mapped to  $\gcd(N_x, M)$  copies of the  $M = 1$  model. Because the interaction Hamiltonian Eq. (4) does not couple different copies, the many-body physics in this case is equivalent to distributing  $N$  on-site interacting particles in  $\gcd(N_x, M)$  decoupled copies of  $M = 1$  models, each with

$[N_x/\gcd(N_x, M)] \times N_y$  unit cells. We can count the zero-energy states straightforwardly by this many-body mapping. For  $\nu = k/2$  with  $N$  is divisible by  $\gcd(N_x, M)$ , we have  $N/\gcd(N_x, M)$  on-site interacting particles at  $\nu = k/2$  in each copy of the  $M = 1$  model. If  $N/\gcd(N_x, M)$  is divisible by  $k$ , this gives us  $k + 1$  zero-energy states obeying the same exclusion rule as the Read-Rezayi states within each copy, and hence a total of  $(k + 1)^{\gcd(N_x, M)}$  zero-energy states. However, when  $N$  is not divisible by  $\gcd(N_x, M)$ , the filling fraction is larger than  $k/2$  in at least one copy, thus there are no zero-energy states [48]. That the degeneracy depends on  $N_x$  but not on  $N_y$  is a striking signature of the nematic nature of these states [7]. Furthermore, the number of particles  $N$  does not necessarily need to be a multiple of  $C = M$ , which further distinguishes the nematic model FCIs from their continuum multi-layer relatives.

*Other states.* Following the constructions detailed above, it is straightforward to construct parent Hamiltonians for an entire zoo of new model FCIs. For instance, for  $M = 2$  and even  $N_x$ , Eq. (6) has a bilayer FQH system as the continuum counterpart. Thus with an on-site inter-orbital three-body repulsion in combination with a two-body intra-orbital repulsion is expected to mimic the parent Hamiltonian for the coupled Moore-Read state [57, 58] in the continuum. The degeneracy of this state on the torus is  $2N + 3$  for even number of particles [59] which is consistent with our numerics [48].

*Discussion.* In this work we have introduced *model fractional Chern insulators*—topologically ordered states with an infinite entanglement gap—and constructed their concomitant local parent Hamiltonians directly in the lattice. Our construction provides natural FCI counterparts of the AKLT model for the Haldane spin chain, the Kitaev chain and the model quantum Hall wave functions and their associated continuum parent Hamiltonians. In analogy with these models, our construction also carries a notion of frustration-freeness in that the ground states reside entirely within the lowest band, and exactly minimize a strictly local  $(k + 1)$ -body repulsions term by term. However, rooted in the impossibility of local Wannier functions for Chern bands [60], it appears impossible to write a gapped parent Hamiltonian, including both interactions and kinetic part, entirely as a sum of positive local terms such that each of them is minimized by the model FCIs in the two-dimensional limit,  $N_x, N_y \rightarrow \infty$  [61–63].

We have conclusively shown that our model provides an infinite gap in the particle entanglement spectrum and that the energy gap remains finite in the thermodynamic limit. These results are particularly remarkable considering the strong lattice effects, e.g. reflected in a strongly non-uniform Berry curvature at small  $\phi$ , and underscores the incompleteness of any long-wave length description of FCIs [1].

Our construction extends the list of FCIs far beyond those in the existing literature. Notably the  $k = 3$ -states (Fig. 2) are the first reported  $C > 1$  higher Chern number generalizations of the Fibonacci anyon quantum Hall states. Moreover, the nematic higher Chern number states provides a particularly promising basis for investigating lattice dislocations, which

have been predicted to behave like non-Abelian wormholes in nematic Abelian parent states [7]. Abelian nematic states have been previously found in Refs. [18, 39]; our construction is giving an ideal realization in contrast to Ref. [18], and is much simpler than the proposed parent Hamiltonian of Ref. [39] which includes a long tail of two-body interactions. Our non-Abelian nematic states are entirely new.

Our model also provides an ideal ground for investigating alternative platforms for Fibonacci anyons, deriving from more elementary Abelian FCIs in proximity to superconductors [64]. In particular, our  $C = 2, k = 1, \nu = 1/3$  provides an ideal lattice version of the (221)-Halperin state which is a key ingredient in the construction considered in Ref. [64].

Finally, our construction provides a guide for designing experimental implementations of FCIs, particularly in cold atom or molecule systems [65] or in arrays of qubits or nonlinear optical resonators [66, 67]. The very recent observation of higher Chern numbers in photonic crystals is highly encouraging in this respect [68].

This work was supported by DFG’s Emmy Noether program (BE 5233/1-1) and by the Dahlem Research School (DRS). Z. L. thanks Nicolas Regnault for related work. Z. L. was additionally supported by the Department of Energy, Office of Basic Energy Sciences through Grant No. DE-SC0002140.

---

\* zliu@zedat.fu-berlin.de

† ejb@physik.fu-berlin.de

- [1] S. A. Parameswaran, R. Roy, and S. L. Sondhi, *Fractional quantum Hall physics in topological flat bands*, *C. R. Physique* **14**, 816 (2013).
- [2] E.J. Bergholtz and Z. Liu, *Topological Flat Band Models and Fractional Chern Insulators*, *Int. J. Mod. Phys. B* **27**, 1330017 (2013).
- [3] T. Neupert, C. Chamon, T. Iadecola, L. H Santos and C. Mudry, *Fractional (Chern and topological) insulators*, *Physica Scripta*, **T164**, 014005 (2015).
- [4] C.-Z. Chang *et al.*, *Experimental Observation of the Quantum Anomalous Hall Effect in a Magnetic Topological Insulator*, *Science* **340**, 6129 (2013).
- [5] G. Jotzu, *et al.*, *Experimental realization of the topological Haldane model with ultracold fermions*, *Nature* **515**, 237 (2014).
- [6] Z. Liu, E.J. Bergholtz, H. Fan, and A.M. Läuchli, *Fractional Chern Insulators in Topological Flat bands with Higher Chern Number*, *Phys. Rev. Lett.* **109**, 186805 (2012).
- [7] M. Barkeshli and X.-L. Qi, *Topological Nematic States and Non-Abelian Lattice Dislocations*, *Phys. Rev. X* **2**, 031013 (2012).
- [8] F. Wang and Y. Ran, *Nearly flat band with Chern number  $C = 2$  on the dice lattice*, *Phys. Rev. B* **84**, 241103(R) (2011).
- [9] M. Trescher and E. J. Bergholtz, *Flat bands with higher Chern number in pyrochlore slabs*, *Phys. Rev. B* **86**, 241111(R) (2012).
- [10] S. Yang, Z.-C. Gu, K. Sun, and S. Das Sarma, *Topological flat band models with arbitrary Chern numbers*, *Phys. Rev. B* **86**, 241112(R) (2012).



- [11] Y.-F. Wang, H. Yao, C.-D. Gong, and D. N. Sheng, *Fractional Quantum Hall Effect in Topological Flat Bands with Chern Number Two*, *Phys. Rev. B* **86**, 201101(R) (2012).
- [12] A. Sterdyniak, C. Repellin, B. Andrei Bernevig, and N. Regnault, *Series of Abelian and non-Abelian states in  $C > 1$  fractional Chern insulators*, *Phys. Rev. B* **87**, 205137 (2013).
- [13] A. G. Grushin, T. Neupert, C. Chamon, and C. Mudry, *Enhancing the stability of fractional Chern insulators against competing phases*, *Phys. Rev. B* **86**, 205125 (2012).
- [14] Y.-L. Wu, N. Regnault and B. A. Bernevig, *Bloch Model Wave Functions and Pseudopotentials for All Fractional Chern Insulators*, *Phys. Rev. Lett.* **110**, 106802 (2013).
- [15] G. Möller and N.R. Cooper, *Composite Fermion Theory for Bosonic Atoms in Optical Lattices*, *Phys. Rev. Lett.* **103**, 105303 (2009).
- [16] D. Wang, Z. Liu, J. Cao, and H. Fan, *Tunable Band Topology Reflected by Fractional Quantum Hall States in Two-Dimensional Lattices*, *Phys. Rev. Lett.* **111**, 186804 (2013).
- [17] N. R. Cooper and R. Moessner, *Designing Topological Bands in Reciprocal Space*, *Phys. Rev. Lett.* **109**, 215302 (2012).
- [18] Y.-H. Wu, J. K. Jain, and K. Sun, *Fractional Topological Phases in Generalized Hofstadter Bands with Arbitrary Chern Numbers*, *Phys. Rev. B* **91**, 041119(R) (2015).
- [19] T. Scaffidi and S. H. Simon, *Exact solutions of fractional Chern insulators: Interacting particles in the Hofstadter model at finite size*, *Phys. Rev. B* **90**, 115132 (2014).
- [20] M. Udagawa and E.J. Bergholtz, *Correlations and entanglement in flat band models with variable Chern numbers*, *J. Stat. Mech.* P10012 (2014).
- [21] E. J. Bergholtz, Z. Liu, M. Trescher, R. Moessner, and M. Udagawa, *Topology and Interactions in a Frustrated Slab: Tuning from Weyl Semimetals to  $C > 1$  Fractional Chern Insulators*, *Phys. Rev. Lett.* **114**, 016806 (2015).
- [22] D. Peter, *et. al.*, *Topological bands with a Chern number  $C = 2$  by dipolar exchange interactions*, *Phys. Rev. A* **91**, 053617 (2015).
- [23] Y.-L. Wu, N. Regnault, and B. A. Bernevig, *Haldane statistics for fractional Chern insulators with an arbitrary Chern number*, *Phys. Rev. B* **89**, 155113 (2014).
- [24] M. Claassen, C. H. Lee, R. Thomale, X.-L. Qi, and T. P. Devereaux, *Position-Momentum Duality and Fractional Quantum Hall Effect in Chern Insulators*, *Phys. Rev. Lett.* **114**, 236802 (2015).
- [25] G. Möller and N. R. Cooper, *Fractional Chern Insulators in Harper-Hofstadter Bands with Higher Chern Number*, *Phys. Rev. Lett.* **115**, 126401 (2015).
- [26] A. Sterdyniak, N. R. Cooper, and N. Regnault, *Bosonic Integer Quantum Hall Effect in Optical Flux Lattices*, *Phys. Rev. Lett.* **115**, 116802 (2015).
- [27] Y.-C. He, S. Bhattacharjee, R. Moessner, and F. Pollmann, *Bosonic Integer Quantum Hall Effect in an Interacting Lattice Model*, *Phys. Rev. Lett.* **115**, 116803 (2015).
- [28] A.M. Läuchli, Z. Liu, E.J. Bergholtz, and R. Moessner, *Hierarchy of fractional Chern insulators and competing compressible states*, *Phys. Rev. Lett.* **111**, 126802 (2013).
- [29] S. Kourtis, J. W. F. Venderbos, and M. Daghofer, *Fractional Chern insulator on a triangular lattice of strongly correlated  $t_{2g}$  electrons*, *Phys. Rev. B* **86**, 235118 (2012).
- [30] E. Kapit and E. Mueller, *Exact Parent Hamiltonian for the Quantum Hall States in a Optical Lattice*, *Phys. Rev. Lett.* **105**, 215303 (2010).
- [31] X.-L. Qi, *Generic Wavefunction Description of Fractional Quantum Anomalous Hall States and Fractional Topological Insulators*, *Phys. Rev. Lett.* **107**, 126803 (2011).
- [32] Y.-L. Wu, N. Regnault, and B.A. Bernevig, *Gauge-Fixed Wannier Wave-Functions for Fractional Topological Insulators*, *Phys. Rev. B* **86**, 085129 (2012).
- [33] Z. Liu and E.J. Bergholtz, *From fractional Chern insulators to Abelian and non-Abelian fractional quantum Hall states: adiabatic continuity and orbital entanglement spectrum*, *Phys. Rev. B* **87**, 035306 (2013).
- [34] T. Scaffidi and G. Möller, *Adiabatic continuation of Fractional Chern Insulators to Fractional Quantum Hall States*, *Phys. Rev. Lett.* **109**, 246805 (2012).
- [35] Y.-H. Wu, J.K. Jain, and K. Sun, *Adiabatic Continuity Between Hofstadter and Chern Insulators*, *Phys. Rev. B* **86**, 165129 (2012).
- [36] M. Greiter, D. F. Schroeter, and R. Thomale, *Parent Hamiltonian for the non-Abelian chiral spin liquid*, *Phys. Rev. B* **89**, 165125 (2014).
- [37] I. Glasser, J. I. Cirac, G. Sierra, G. and A. E. B. Nielsen, *Exact parent Hamiltonians of bosonic and fermionic Moore-Read states on lattices and local models*, *New Journal of Physics*, **17** 082001 (2015).
- [38] Z. Liu, E. J. Bergholtz and E. Kapit, *Non-Abelian fractional Chern insulators from long-range interactions*, *Phys. Rev. B* **88**, 205101 (2013).
- [39] C. H. Lee and X.-L. Qi, *Lattice construction of pseudopotential Hamiltonians for fractional Chern insulators*, *Phys. Rev. B* **90**, 085103 (2014).
- [40] I. Affleck, T. Kennedy, E. H. Lieb, and H. Tasaki, *Rigorous results on valence-bond ground states in antiferromagnets*, *Phys. Rev. Lett.* **59**, 799 (1987).
- [41] A. Kitaev, *Unpaired Majorana fermions in quantum wires*, *Phys. Usp.* **44**, 131 (2001).
- [42] R.B. Laughlin, *Anomalous Quantum Hall Effect: An Incompressible Quantum Fluid with Fractionally Charged Excitations*, *Phys. Rev. Lett.* **50**, 1395 (1983).
- [43] G. Moore, and N. Read, *Nonabelions in the fractional quantum Hall effect*, *Nucl. Phys. B* **360**, 362 (1991).
- [44] N. Read and E. Rezayi, *Beyond paired quantum Hall states: Parafermions and incompressible states in the first excited Landau level*, *Phys. Rev. B* **59**, 8084 (1999).
- [45] F.D.M. Haldane, *Fractional Quantization of the Hall Effect: A Hierarchy of Incompressible Quantum Fluid States*, *Phys. Rev. Lett.* **51**, 605 (1983).
- [46] A. Sterdyniak, N. Regnault, and B. A. Bernevig, *Extracting Excitations from Model State Entanglement*, *Phys. Rev. Lett.* **106**, 100405 (2011).
- [47] N. Regnault and B. A. Bernevig, *Fractional Chern Insulator*, *Phys. Rev. X* **1**, 021014 (2011).
- [48] See the Supplementary Material for (i) the detailed description of our model, and (ii) the ground state degeneracy for various samples and interaction types.
- [49] For a finite periodic lattice, we need to extend  $t_{j,k}^{s_j,s_k}$  to its magneto-periodic version. See Ref. [30] for an example of  $M = 1$ .
- [50] L. Chen, T. Mazaheri, A. Seidel, and X. Tang, *The impossibility of exactly flat non-trivial Chern bands in strictly local periodic tight binding models*, *J. Phys. A: Math. Theor.* **47**, 152001 (2014).
- [51] For a few very small system sizes, for example  $N = 2$ ,  $N_x \times N_y = 2 \times 2$ ,  $M = 1$ ,  $k = 1$ ,  $\phi = 1/2$  and  $N = 4$ ,  $N_x \times N_y = 2 \times 2$ ,  $M = 1$ ,  $k = 2$ ,  $\phi = 1/2$ , we observe more zero modes than expected. These disappear by slightly increasing  $N$  or decreasing  $\phi$ .
- [52] Each eigenstate can be labeled by a two-dimensional total quasi-momentum  $(K_x, K_y)$ . The ground state degeneracy is

- not always possible to resolve for  $d = 1$ . In that case, we select the same number of lowest states in each  $(K_x, K_y)$  sector as the  $d = \infty$  case to construct the ground state manifold  $\{|\Psi_\alpha\rangle\}$ .
- [53] Yang-Le Wu, B. Andrei Bernevig, and N. Regnault, *Zoology of fractional Chern insulators*, *Phys. Rev. B* **85**, 075116 (2012).
  - [54] B. I. Halperin, *Theory of the Quantized Hall Conductance*, *Helv. Phys. Acta* **56**, 75 (1983).
  - [55] E. Ardonne and K. Schoutens, *New Class of Non-Abelian Spin-Singlet Quantum Hall States*, *Phys. Rev. Lett.* **82**, 5096 (1999).
  - [56] E. Ardonne, N. Read, E. Rezayi, and K. Schoutens, *Non-abelian spin-singlet quantum Hall states: wave functions and quasihole state counting*, *Nucl. Phys. B* **607**, 549 (2001).
  - [57] L. Hormozi, G. Möller, and S. H. Simon, *Fractional Quantum Hall Effect of Lattice Bosons Near Commensurate Flux*, *Phys. Rev. Lett.* **108**, 256809 (2012).
  - [58] Gunnar Möller, Layla Hormozi, Joost Slingerland, and Steven H. Simon, *Josephson-coupled Moore-Read states*, *Phys. Rev. B* **90**, 235101 (2014).
  - [59] Z. Liu, A. Vaezi, C. Repellin, and N. Regnault, *Phase diagram of  $\nu = \frac{1}{2} + \frac{1}{2}$  bilayer bosons with inter-layer couplings*, *Phys. Rev. B* **93**, 085115 (2016).
  - [60] D. J. Thouless, *Wannier functions for magnetic sub-bands*, *J. Phys. C* **17**, L325 (1984).
  - [61] J. Dubail and N. Read, *Tensor network trial states for chiral topological phases in two dimensions and a no-go theorem in any dimension*, *Phys. Rev. B* **92**, 205307 (2015).
  - [62] T.B. Wahl, H.-H. Tu, N. Schuch, and J.I. Cirac, *Projected entangled-pair states can describe chiral topological states*, *Phys. Rev. Lett.* **111**, 236805 (2013).
  - [63] Constructing quasi-local parent Hamiltonians may however be possible, but remains a significant challenge. Moreover, if say  $N_x$  remains finite an exponentially localised parent Hamiltonian can be constructed.
  - [64] R. S. K. Mong, *et. al.* *Universal topological quantum computation from a superconductor/Abelian quantum Hall heterostructure*, *Phys. Rev. X* **4**, 011036 (2014).
  - [65] I. Bloch, J. Dalibard, and W. Zwerger, *Many-body physics with ultracold gases*, *Rev. Mod. Phys.* **80**, 885 (2008).
  - [66] M. Hafezi, E. A. Demler, M. D. Lukin, and J. M. Taylor, *Robust optical delay lines with topological protection*, *Nat. Phys.* **7**, 907 (2011).
  - [67] E. Kapit, M. Hafezi, and S. H. Simon, *Induced Self-Stabilization in Fractional Quantum Hall States of Light*, *Phys. Rev. X* **4**, 031039 (2014).
  - [68] Scott A. Skirlo, Ling Lu, Yuichi Igarashi, Qinghui Yan, John Joannopoulos, and Marin Soljačić, *Experimental Observation of Large Chern Numbers in Photonic Crystals*, *Phys. Rev. Lett.* **115**, 253901 (2015).

## SUPPLEMENTARY MATERIAL

In this Supplementary Material, we first discuss our flat band model with more details. We furthermore provide the ground state degeneracy (GSD), i.e. the number of zero modes, obtained by numerical diagonalization of the interaction Hamiltonian for various samples and interaction types.

## FLAT BAND MODEL

In the main text, we consider a square lattice with an effective magnetic flux  $\phi = 1/q$  piercing each elementary plaquette. We assign  $M$  internal orbitals to each lattice site  $i$  with the real-space coordinate  $(x_i, y_i)$ , where  $M$  must be a factor of  $q$ . We then label each orbital by a site-dependent index

$$s_i = x_i \bmod \left(\frac{q}{M}\right) + m \frac{q}{M}, \quad (5)$$

with  $m = 0, 1, \dots, M - 1$ , such that orbitals with indices in the same residue class  $s_i \equiv s_k \bmod \left(\frac{q}{M}\right)$  share the same lattice site. The single-particle tight-binding Hamiltonian is

$$H_0 = \sum_{j,s_j} \sum_{k,s_k} t_{j,k}^{s_j,s_k} a_{j,s_j}^\dagger a_{k,s_k}, \quad (6)$$

where  $a_{j,s_j}^\dagger$  ( $a_{j,s_j}$ ) creates (annihilates) a particle on the orbital  $s_j$  at site  $j$ . To achieve an exactly flat lowest Chern band with Chern number  $\mathcal{C} = M$ , we choose the hopping amplitudes as

$$t_{j,k}^{s_j,s_k} = \delta_{s_j-x_j,s_k-x_k}^{\bmod q} (-1)^{x+y+xy} e^{-\frac{\pi}{2}(1-\phi)|z|^2} e^{-i\pi\phi(\tilde{x}_j+\tilde{x}_k)y}, \quad (7)$$

where  $z_j = x_j + iy_j$ ,  $z = z_j - z_k$ , and  $\tilde{x}_j = x_j + (s_j - x_j) \bmod q$ .

In Fig. 4, we show typical examples of our model for  $\phi = 1/2$ ,  $M = 2$ ;  $\phi = 1/3$ ,  $M = 3$ ; and  $\phi = 1/4$ ,  $M = 2$ . Once  $\phi$  and  $M$  are fixed, the orbital index  $s_i$  in each lattice site can be easily computed from Eq. (5). For example, for  $\phi = 1/4$ ,  $M = 2$ , Eq. (5) gives  $s_i = (x_i \bmod 2) + 2m$ ,  $m = 0, 1$ . So we have  $s_i = 0, 2$  for even  $x_i$  and  $s_i = 1, 3$  for odd  $x_i$  (lower panel in Fig. 4). The unit cell, which contains  $q/M$  sites, can be determined by the period of orbital indices. Hopping only occurs between orbitals satisfying  $(s_j - x_j) \bmod q = (s_k - x_k) \bmod q$  due to the  $\delta_{s_j-x_j,s_k-x_k}^{\bmod q}$  factor in Eq. (7). If we imagine all orbitals that can be connected by hopping as an effective “layer”, it is obvious to see that our model on an infinite lattice is

Table I. The ground state degeneracy (GSD), i.e. the number of zero modes, obtained by numerical diagonalization of the interaction Hamiltonian for various samples and interaction types. As discussed in the main paper, here we consider color-entangled FCIs, nematic FCIs, and other states (separated by the horizontal lines). The notations of symbols are the same as in the main paper. “N/A” means that we do not include the specific interaction type.

$N$	$N_x \times N_y$	$M$ ( $C = M$ )	$\gcd(N_x, M)$	$\phi$	$\nu$	intra-orbital interaction	inter-orbital interaction	GSD
6	$6 \times 3$	2	2	$1/2$	$1/3$	$k = 1$	$k = 1$	3
7	$3 \times 7$	2	1	$1/2$	$1/3$	$k = 1$	$k = 1$	3
6	$3 \times 3$	2	1	$1/2$	$2/3$	$k = 2$	$k = 2$	6
8	$4 \times 3$	2	2	$1/2$	$2/3$	$k = 2$	$k = 2$	6
9	$3 \times 3$	2	1	$1/2$	1	$k = 3$	$k = 3$	10
6	$6 \times 4$	3	3	$1/3$	$1/4$	$k = 1$	$k = 1$	4
7	$4 \times 7$	3	1	$1/3$	$1/4$	$k = 1$	$k = 1$	4
6	$3 \times 4$	3	3	$1/3$	$1/2$	$k = 2$	$k = 2$	10
8	$4 \times 4$	3	1	$1/3$	$1/2$	$k = 2$	$k = 2$	10
9	$3 \times 4$	3	3	$1/3$	$3/4$	$k = 3$	$k = 3$	20
6	$3 \times 4$	2	1	$1/2$	$1/2$	$k = 1$	N/A	2
8	$4 \times 4$	2	2	$1/2$	$1/2$	$k = 1$	N/A	4
6	$6 \times 2$	4	2	$1/4$	$1/2$	$k = 1$	N/A	4
7	$2 \times 7$	2	2	$1/2$	$1/2$	$k = 1$	N/A	0
6	$3 \times 2$	2	1	$1/2$	1	$k = 2$	N/A	3
8	$2 \times 4$	2	2	$1/4$	1	$k = 2$	N/A	9
10	$2 \times 5$	2	2	$1/2$	1	$k = 2$	N/A	1
9	$2 \times 3$	2	2	$1/4$	$3/2$	$k = 3$	N/A	0
12	$2 \times 4$	2	2	$1/4$	$3/2$	$k = 3$	N/A	16
6	$2 \times 6$	2	2	$1/2$	$1/2$	$k = 2$	$k = 1$	15
8	$4 \times 4$	2	2	$1/2$	$1/2$	$k = 2$	$k = 1$	19

equivalent to the stacking of  $M$  “layers” of the  $M = 1$  model (Fig. 4). However, the phase of the hopping between two specific lattice sites is layer-dependent. This can be seen from the Aharonov-Bohm factor  $e^{-i\pi\phi(\tilde{x}_j+\tilde{x}_k)y}$  in Eq. (7), where  $\tilde{x}_j$  is shifted from the site coordinate  $x_j$  by an orbital (layer)-dependent term  $(s_j - x_j) \bmod q$ . For example, if we consider the hopping from site  $(x_k, y_k) = (0, 0)$  to  $(x_j, y_j) = (0, 1)$  in the upper panel of Fig. 4, a phase  $e^{i0}$  ( $e^{i\pi}$ ) is picked up because  $\tilde{x}_j = \tilde{x}_k = 0$  ( $\tilde{x}_j = \tilde{x}_k = 1$ ) in the blue (red) layer. The factor  $\delta_{s_j-x_j, s_k-x_k}^{\bmod q}$  in Eq. (7) guarantees that the shift term  $(s_j - x_j) \bmod q$  is constant in each layer. When  $M = 1$ , we have  $s_i = x_i \bmod q$  which leads to  $\delta_{s_j-x_j, s_k-x_k}^{\bmod q} = 1$  and  $\tilde{x}_i = x_i$ . Thus our model returns to the Kapit-Mueller model [30] in Landau gauge. If we only keep the nearest neighbor hopping, the phase shift differentiates our model from the usual multi-orbital Hofstadter model, where the hopping phase only depends on the lattice site coordinate thus no phase shift exists. Instead, our model can be thought as a multi-orbital Hofstadter model with the orbital-dependent hopping phase and color-entangled boundary condition.

Although it is straightforward on an *infinite* lattice to map our model to the shifted stacking of  $M$  layers of the  $M = 1$  model, a *finite* lattice of  $N_x \times N_y$  unit cells with simple periodic boundary conditions can lead to complicated boundary conditions in the layer stacking picture. Let us consider an example with  $\phi = 1/2, M = 2$  (Fig. 5). If  $N_x$  is even, by tracking the nearest-neighbor hopping in the  $x$  direction, we can find that all hopping still occurs between orbitals with the same color (i.e., the same effective layer). In that case, our model is again equivalent to the shifted stacking of two complete  $M = 1$  layers, each of which has integer number of unit cells and periodic boundary conditions (left panel of Fig. 5). However, if  $N_x$  is odd, Eq. (7) leads to  $x$ -direction hopping between orbitals with different colors across the boundary (right panel of Fig. 5), which implements color-entangled boundary conditions [7,14,18] in the  $x$ -direction for the two effective layers. Crucially, each layer is no longer a complete  $M = 1$  model with integer number of unit cells and periodic boundary conditions. Instead, by unfolding the two layers, our model is now equivalent to a single copy of  $M = 1$  model with usual periodic boundary conditions. In general, one can find that our model on a periodic  $N_x \times N_y$  lattice can be mapped to  $\gcd(N_x, M)$  copies of complete  $M = 1$  model with usual periodic boundary conditions, each copy has  $[N_x / \gcd(N_x, M)] \times N_y$  unit cells and copy-dependent Aharonov-Bohm hopping phases.

## GROUND STATE DEGENERACY

Here we summarize the ground state degeneracy, i.e. the number of zero modes, obtained by numerical diagonalization of the interaction Hamiltonian for various samples and interaction types (Tab. I).

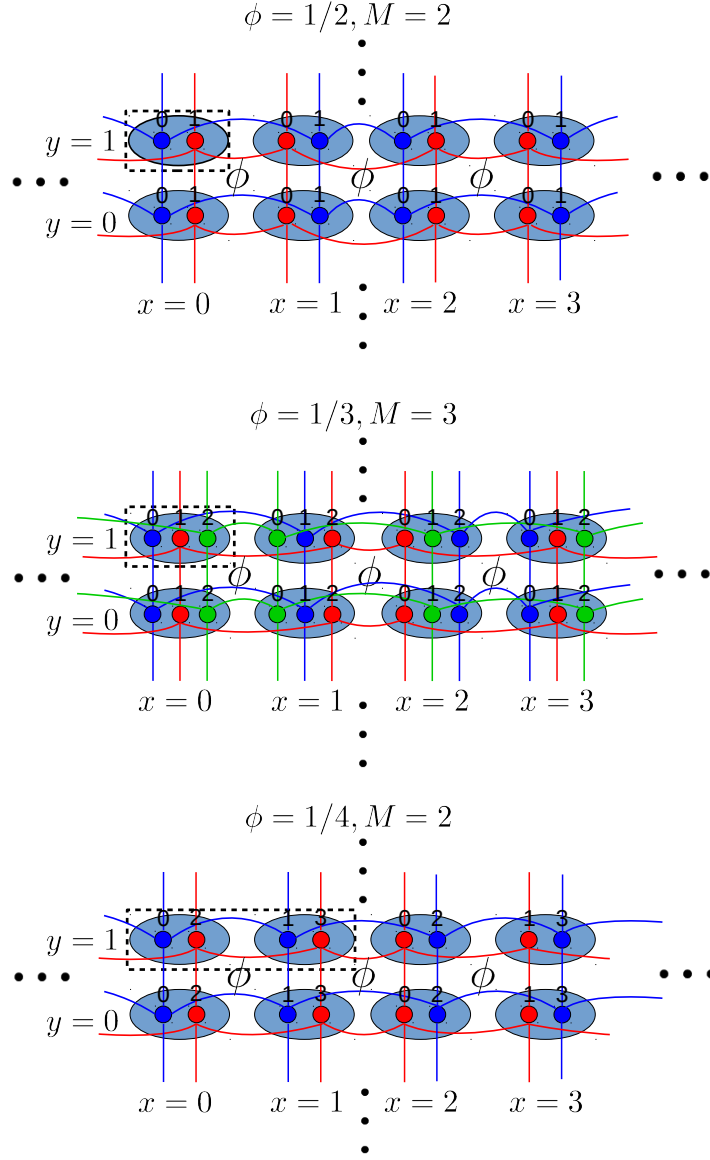


Figure 4. Typical examples of our flat band model for different  $\phi = 1/q$  and  $M$ . Each ellipse represents a lattice site with the real-space coordinate  $(x, y)$ . In each lattice site  $i$ , there are circles representing orbitals, whose indices  $s_i$  are given by the numbers. The orbitals connected by allowed hopping (only nearest-neighbor hopping is shown for simplicity) in Eq. (7) have the same color and can be thought as an effective layer. The unit cell containing  $q/M$  sites is indicated by the dashed rectangular. In the infinite lattice case, our model is equivalent to the stacking of  $M$  layers of the  $M = 1$  model, with layer-dependent Aharonov-Bohm hopping phases.



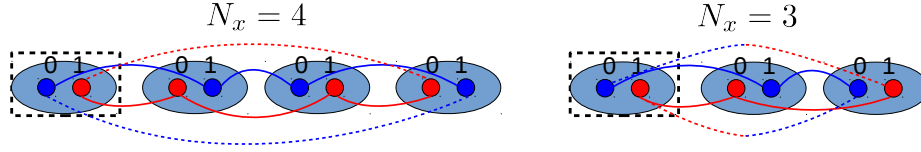


Figure 5. Our model on periodic finite lattices with  $\phi = 1/2$  and  $M = 2$ . The unit cell is indicated by the dashed rectangular. The hopping across the boundary is highlighted by the dashed lines. (a) When  $N_x = 4$ , our model is equivalent to two (blue and red) complete  $M = 1$  layers with periodic boundary conditions. (b) When  $N_x = 3$ , hopping across the boundary may occur between orbitals (layers) with different colors. Thus we have color-entangled boundary conditions in the  $x$ -direction for the blue and red layers, and each layer is no longer a complete  $M = 1$  model with integer number of unit cells and periodic boundary conditions.